

Mars Soil Temperature and Thermal Properties from InSight HP³ Data

T. Spohn¹, N. Müller¹, J. Knollenberg¹, M. Grott¹, M. P. Golombek², A.-C.
Plesa¹, V. T. Bickel³, P. Morgan⁴, C. Krause⁵, D. Breuer¹, S. E. Smrekar², W.
B. Banerdt^{2*}

¹Institute of Planetary Research, German Aerospace Center DLR, Rutherfordstrasse 2, 12489 Berlin,
Germany

²Jet Propulsion Laboratory, California Institute of Technology, 4800 Oak Grove Drive, Pasadena, Ca
91109, USA

³Center for Space and Habitability, University of Bern, Gesellschaftsstrasse 6, 3012 Bern, Switzerland

⁴Colorado Geological Survey, Colorado School of Mines, 1801 19th St., Golden, Co 80401, USA

⁵MUSC Space Operations and Astronaut Training, German Aerospace Center DLR, Linder Höhe, 51147
Köln, Germany

Key Points:

- We measured the temperature and its diurnal and annual variations in the top 40cm of the Martian soil at the InSight landing site
- The soil temperature allows the formation of thin films of brine; its deliquescence may explain the formation of the observed duricrust
- The soil thermal diffusivity was calculated from the diurnal and annual surface and soil temperature variations and increases with depth

*current address: 1854 Clayton Ave. Pittsburg, Pa 15214, USA

Corresponding author: Tilman Spohn, tilman.spohn@dlr.de

Abstract

Temperature is of primary importance for many physical properties in the Martian soil. We measured diurnal and annual soil (and surface) temperature variations using the NASA InSight Mars mission's HP³ radiometer and thermal probe. At the depth of the probe of 0.5 - 36cm, an average temperature of 217.5 K was found varying by 5.3 - 6.7 K during a sol and by 13.2 K during the seasons. The damping of the surface temperature variations in the soil were used to derive a thermal diffusivity of $2.30 \pm 0.03 \times 10^{-8} \text{ m}^2/\text{s}$ for the depth range of the diurnal wave - thermal skin depth $2.5 \pm 0.04 \text{ cm}$ - and $3.74 \pm 0.61 \times 10^{-8} \text{ m}^2/\text{s}$ for that of the annual wave, with a thermal skin depth of $84 \pm 10 \text{ cm}$. The temperatures measured are conducive to the deliquescence of thin films of brines in the soil. These are of astrobiological interest and may explain the formation of the observed cemented duricrust.

Plain Language Summary

Temperature is of primary importance for many physical properties of the Martian soil as it determines how rapidly physical processes and chemical reactions will proceed, including the transport of heat and materials. Temperature is of particular interest to astrobiology, informing the habitability of the soil and whether water or brine may exist on which microorganisms could live. We measured the temperature in the soil during several Martian days and over a Martian year using the NASA InSight Mars mission's Heat Flow and Physical Properties Package. Over the depth extent of its thermal probe of about 40cm, an average temperature of -56°C was measured, varying by 5 to 7 degrees during the day - only a tenth of the daily surface temperature variation - and by 13 degrees during the seasons. The temperature is subfreezing for water but allows the formation of thin films of salty brine for 10h or more during a Martian day. The solidification of the brine could have caused cementation of the soil and explain the observed few tens of cm thick duricrust, a layer of consolidated, cohesive sand, which is thought to have hampered the penetration to greater depth of the mission's thermal probe.

1 Introduction

The temperature in the Martian soil has been estimated but is mostly unknown. Orbiter and surface lander and rover missions have measured the surface temperature and thermal inertia but the temperature in the soil at more than millimeters depth has

52 never before been measured. (Compare the near-surface soil temperatures measured by
53 the Phoenix TECP instrument using a 15 mm long spike sensor, e.g., Zent et al. (2010).)
54 Soil temperature is of primary importance for the values of physical properties such as
55 elasticity, seismic velocity, thermal conductivity and heat capacity, which are temper-
56 ature dependent (e.g., Morgan et al., 2018). Its value and the manner in which it varies
57 in time and space determines the rates and directions of soil physical processes and of
58 energy and mass exchange with deeper layers and the atmosphere (e.g., Hillel, 2001). More-
59 over, temperature governs the rates of chemical reactions that take place in the soil, in-
60 cluding biological processes and is of particular interest to astrobiology (e.g., Jones et
61 al., 2011) and future human exploration (e.g., Rapp, 2023). For life to flourish in the sub-
62 surface, temperature needs to be above the freezing point of water or the eutectic tem-
63 perature of brine that may be contained in the soil and used as essential solvents by or-
64 ganisms (e.g., Cockell, 2014).

65 Soil temperature varies in time and space driven mostly by changes at the surface
66 and the transport of heat in the soil by solid state heat conduction, heat advection through
67 gas transport and latent heat exchange upon e.g., freezing and thawing. Heat transport
68 in the Martian soil has been modelled by e.g., Grott et al. (2007) but because of the com-
69 plex transport processes in the soil and the temperature dependence of material param-
70 eters, modeling of the thermal regime is a formidable task. Here, we report the first mea-
71 surement of soil temperature at a depth of up to 36cm using the Nasa InSight Mars mis-
72 sion’s Heat Flow and Physical Properties Package HP³. Even though we measured soil
73 temperature only at one location on Mars close to the equator, the data can serve as a
74 valuable reference for future modeling and to inform astrobiological considerations and
75 simulation experiments (e.g., Boston et al., 2009). By comparing the amplitude and phase
76 of the sub-surface with the surface temperature we calculated the thermal diffusivity of
77 the soil.

78 The HP³ package was originally planned to measure the planetary surface heat flow
79 and the thermal and mechanical properties of the Martian soil up to 5 m depth (Spohn
80 et al., 2018). The mission has been described in e.g., Banerdt et al. (2020); the landing
81 site and its Geology have been described in Golombek et al. (2020). The lander is located
82 at 4.502°N, 135.623°E at an elevation of -2,613.43 m with respect to the geoid in what
83 has been informally named *Homestead Hollow* in Elysium Planitia in the Early Hesper-
84 ian Transition unit (Golombek et al., 2020).

85 Temperature sensors printed on a 5m long Kapton™ tether would have been brought
86 to the target depth of 3–5m by a small penetrator, nicknamed the mole. The 40cm long
87 mole which requires friction on its hull to balance remaining recoil from its internal ham-
88 mer mechanism did not penetrate to the targeted depth. The root cause of the failure
89 - as was determined through an extensive, almost one Martian year long campaign de-
90 scribed in detail in Spohn, Hudson, Witte, et al. (2022) and Spohn, Hudson, Marteau,
91 et al. (2022) - was a lack of friction in an unexpectedly thick cohesive - possibly cemented
92 - duricrust. During the recovery campaign, the mole penetrated to a final tip-depth of
93 about 36 cm with an inclination to vertical of 30°, bringing the mole’s back-end about
94 1 cm below the surface. Penetration was aided by friction applied to the mole with the
95 scoop at the end of the robotic Instrument Deployment Arm (Trobi-Ollennu et al., 2018)
96 and by direct support to its back-cap.

97 The penetration record was used to infer a layering of the soil and its thermo-mechanical
98 properties (Spohn, Hudson, Marteau, et al., 2022). Accordingly (compare Fig. 1), a 7–
99 20 cm thick duricrust underlies a 1–2 cm dust layer. Underneath the duricrust is a 10–
100 23 cm thick sand layer followed by a gravel/sand mixture. The duricrust has a penetra-
101 tion resistance of 0.3–0.7 MPa, while the gravel layer (> 30 cm depth) a resistance of
102 4.9 ± 0.4 MPa. Using the mole’s thermal sensors and internal heaters, the average soil
103 temperature, thermal conductivity and the soil density were measured. The average value
104 of the thermal conductivity was found to be 0.039 W/m K (Grott et al., 2021) varying
105 by ± 5 % over the seasons (solar longitude between 8° and 210°) and with atmosphere
106 pressure (Grott et al., 2023). The conductivity likely increases from 0.014 W/m K to 0.034 W/m K
107 through the topmost sand/dust layer, keeping the latter value in the duricrust and the
108 sand layer underneath and then increasing to 0.064 W/m K in the sand/gravel layer (Spohn,
109 Hudson, Marteau, et al., 2022). The density decreases from 1200 kg/m³ in the sand/dust
110 layer to 950–1100 kg/m³ in the duricrust, then increases to 1300–1500 kg/m³ in the sand
111 layer underneath and further to 1600 kg/m³ in the sand/gravel layer.

112 Prior to each thermal conductivity measurement, the soil temperature was recorded
113 for 48h. The diurnal and seasonal variations of the soil temperature are reported in this
114 paper. The data are complemented by housekeeping (H/K) temperature data taken in-
115 side the mole at the motor block at times when the HP³ instrument was powered on.
116 A comparison with the surface temperature allows the calculation of the thermal diffu-
117 sivity and a more precise estimate of the depth to the mole in the soil. The sensors have

118 been described in Spohn et al. (2018) and more specifically in the Supporting Informa-
 119 tion Text S1.

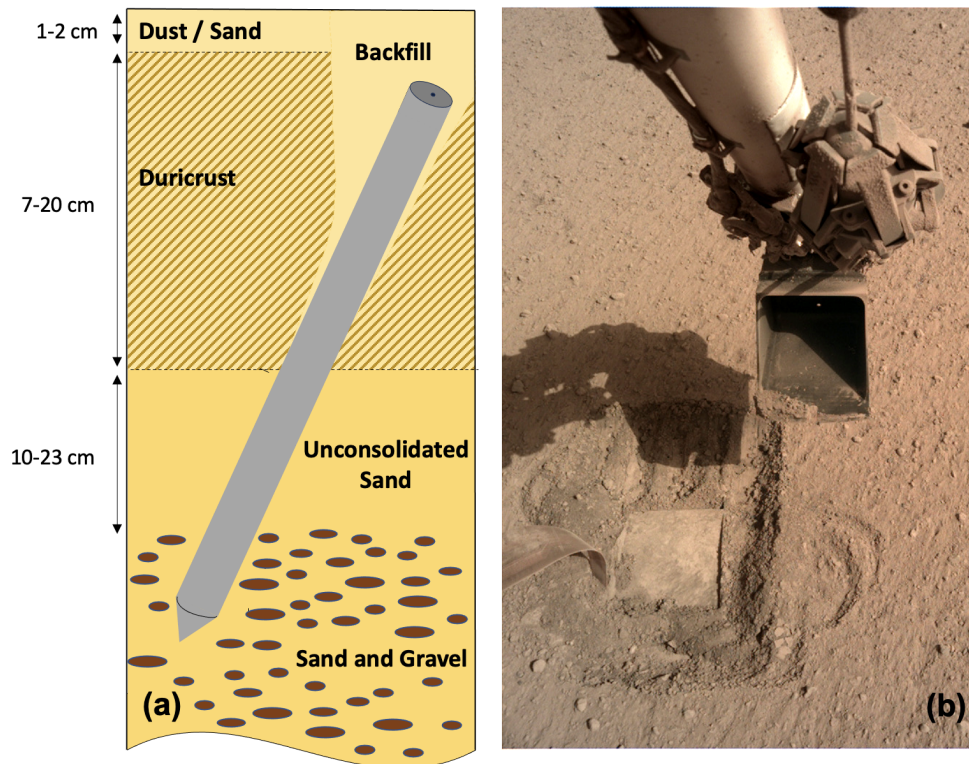


Figure 1. a) Sketch of the mole in the soil and of the soil layering. b) The mole pit filled with soil and compressed with the scoop of the robotic Instrument Deployment Arm (IDA) after sol 754, the sol of the final penetration test. A solar day (sol) on Mars is 24 Mars hours of 61.65 min. The sols are counted starting with the landing of InSight on sol 0.

120 2 Results

121 The first 48h diurnal soil temperature measurement using the TEM-A thermal sen-
 122 sors on the fully buried mole was taken on sol 680, shortly after buriage (Spohn, Hud-
 123 son, Marteau, et al., 2022) on sol 673 but before the soil was tamped on sols 686 and 734
 124 with the robotic arm as in Fig. 1b. On Sol 754, the mole motor was operated to see whether
 125 the mole would penetrate further on its own after being buried and the soil consolidated.
 126 When it failed to clearly penetrate further during a 506 hammer strokes long campaign
 127 - the final "Free Mole Test" - the attempts to bring the mole to greater depth were aban-

128 done because the diminishing resources were needed for other instruments on the mis-
129 sion. The TEM-A measurement on sol 795 was the first measurement after the Free Mole
130 Test hammering. This hammering may have contributed to a further settling and com-
131 paction of the pit fill. The six 48h TEM-A measurements thereafter were all done in the
132 same configuration.

133 Fig. 2 top panel shows the soil temperature as a function of local true solar time
134 LTST and for sols 681–1202. The temperature curves are largely parallel except for sol
135 681. The situation in the soil before the Free Mole Test and the final tamping of the sand
136 scraped into the pit may have contributed to the anomaly. The small rate of increase
137 of temperature after noon of sol 681 was likely caused by the shadow of the scoop which
138 was just above the mole at the time. Moreover, InSight ICC images and camera data
139 (<https://mars.nasa.gov/insight/multimedia/raw-images>, see also Lemmon et al. (2015))
140 suggest that it was a particularly dusty sol at Homestead Hollow.

141 Fig. 2 bottom panel shows the diurnally averaged TEM-A and mole motor house-
142 keeping (H/K) temperature values as a function of time in sols starting with sol 681 and
143 extending to sol 1245, the last sol on which HP³ data were taken. The H/K tempera-
144 tures are consistent with the TEM-A values. In addition, we plot the average of the di-
145 urnal peak values of the surface temperature measured by the RAD sensor (Spohn et
146 al., 2018; Mueller et al., 2020) at surface spot2 (compare Supporting Information Text
147 S1). Spot2 is located opposite to the location of the mole with respect to the lander and
148 is centred at a distance of about 4 m from the center of the lander. The surface temper-
149 ature was recorded during the second InSight Mars year at 6:00 and 13:00 LTST, cov-
150 ering the daily maximum and minimum values. The values plotted in Fig. 2 are the av-
151 erage values between the two. We further plot the 24h-averaged surface temperature for
152 8 sols for which data were taken together with an estimate of the average surface tem-
153 perature calculated from the 6:00 and 13:00 LTST values and using a relation between
154 the 24h-averaged temperature and the average between the peak-to-peak values derived
155 from the data of InSight year 1. Both curves differ notably by 8 K in the winter and by
156 13 K during the summer. The difference is due to the non-symmetry of the variation of
157 the surface temperature during a sol (compare Fig. S3 in the Supporting Information).

158 Temperature in the soil varied by 5.3 K during a sol for the coldest sol sampled,
159 sol 871, to 6.7 K for the warmest sol, sol 1202. Over the seasons, TEM-A 24h-averaged

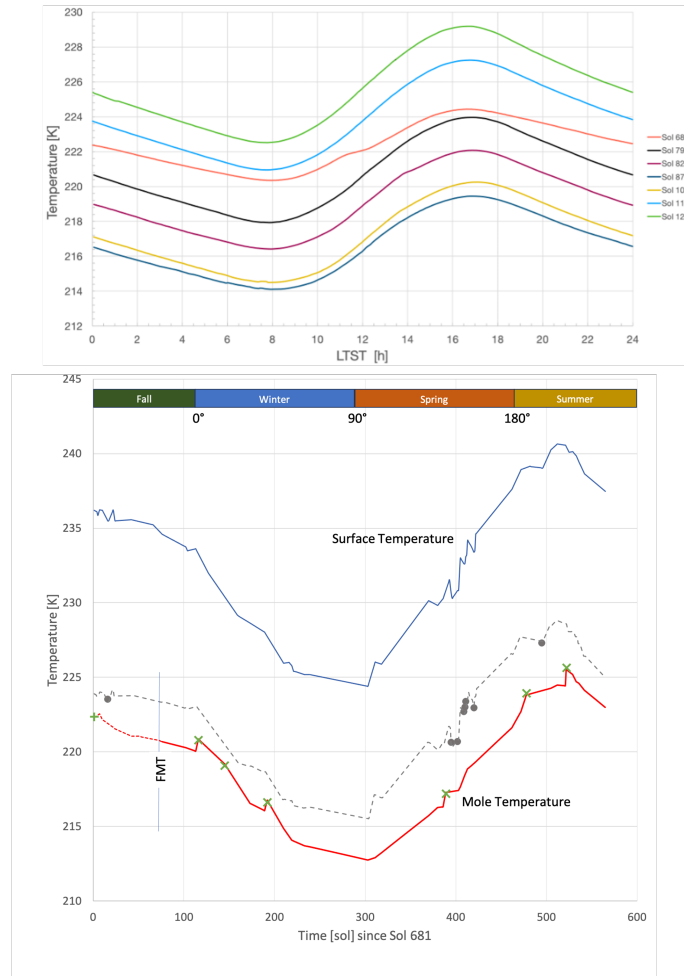


Figure 2. Top: Soil temperature as measured by the TEM-A sensor as a function of local true solar time (LTST) on the sols indicated. The uncertainty of the temperature measured with TEM-A is estimated to be 0.1 K (Grott et al., 2019). Bottom: Surface and TEM-A and mole motor H/K temperatures versus time in Martian solar days (sol). The blue line gives the surface temperature averaged using radiometer readings at 6:00 and 13:00 LTST. Their uncertainty is estimated to be 2 K (Mueller et al., 2020). The grey dots give the available 24h-averaged surface temperatures. Their uncertainty is about 3K, given the uncertainty of up to 6K of temperature measurements in the late afternoon. The dashed grey line gives an estimate of the 24h-averaged temperature using the diurnal minimum and maximum temperatures of year 2 (blue line) and a mapping derived from 24h averages and peak-to-peak averages from year 1. The green crosses give the soil temperature measured by TEM-A from the top panel and averaged over one sol. The red line gives the mole motor H/K temperature, averaged using readings at 6:00 and 13:00 LTST with an uncertainty of 1 K. FMT indicates the sol (754) at which the Free Mole Test occurred. Additionally marked are the Northern hemisphere seasons and the solar longitude.

160 temperatures varied by 9 K from 216.8 K at sol 871 to 225.8 K at sol 1202. Note that
 161 the TEM-A measurements missed the temperature low around sol 980 (211.8 K at sol
 162 981, Fig. 2 bottom) suggesting a temperature difference through the Martian year of 13.3 K.
 163 The annual average temperature calculated from the TEM-A recordings and the H/K
 164 data is 217.5 K. These compare with an annual average surface temperature of 221.6 K.

165 The damping of the diurnal and annual surface temperature variation and the phase
 166 shift with increasing depth can be used to estimate the thermal diffusivity and the depth
 167 to the back-end of the mole. Note that the latter was not well known before but was es-
 168 timated to be 1-2 cm from camera data (Spohn, Hudson, Marteau, et al., 2022). We briefly
 169 describe our calculation here. More detail can be found in the Supporting Information
 170 Text S2.

171 It is well known (e.g., Carslaw & Jaeger, 1959) that the peak-to-peak temperature
 172 oscillation in a half-space heated periodically at the surface decreases with $\exp(z/\delta)$, where
 173 z is depth and where $\delta = \sqrt{\kappa P/\pi}$ is the thermal skin depth, with P the period of the
 174 forcing temperature variation. Averaged over the depth interval sampled by the mole,
 175 we get for the peak-to-peak variation $\overline{\Delta T}$

$$\overline{\Delta T} = \frac{1}{z_1 - z_0} \int_{z_0}^{z_1} \Delta T(z=0) e^{-z/\delta} dz \quad (1)$$

176 where z_0 is the depth to the mole back-end and z_1 the depth to the mole tip. The phase
 177 lag Φ of the temperature variation increases with depth according to z/δ . Because the
 178 temperature signal decreases exponentially along the mole, we calculate the average value
 179 of the phase lag by taking a weighted average over the depth extent of the mole:

$$\overline{\Phi} = \frac{\frac{1}{\delta} \int_{z_0}^{z_1} z e^{-(z-z_0)/\delta} dz}{\int_{z_0}^{z_1} e^{-(z-z_0)/\delta} dz} \quad (2)$$

180 The diurnal and annual thermal skin depths, respectively, are given by:

$$\delta_d = \sqrt{\frac{\kappa P_d}{\pi}} \quad (3)$$

$$\delta_a = \sqrt{\frac{\kappa P_a}{\pi}} \quad (4)$$

181 where P_d is a sol and P_a a Martian year in seconds.

182 For the diurnal wave, we use the six TEM-A 24h recordings available for sols 796
 183 - 1202 as shown in Fig. 2. (We do not use the sol 681 TEM-A recording because it is
 184 quite anomalous, as was discussed further above.) We compare these with 24h surface
 185 temperature recordings from the HP³ radiometer RAD. Unfortunately, these were not
 186 taken on the same sols as the TEM-A recordings. Therefore, we use the next available
 187 sol with 24h RAD data. These are sol 1075 for sol 1069 and sol 1175 for sol 1157. For
 188 sols 796, 825, 872 and 1202, we use data from a close-by sol with similar solar longitude
 189 of the previous Martian year. These are sol 120 (for 796), sol 138 (825), sol 190 (872)
 190 and sol 511 (1202). Although InSight year 2 on Mars was overall cooler by a few Kelvin
 191 than year 1, the diurnal temperature variations were very similar. Fig. 3 shows the so-
 192 lutions to Eqns. 1 and 2 in terms of z_0 and κ after de-trending for - albeit small - de-
 193 pendencies of the measured amplitude ratio and phase lag on the surface temperature
 194 and of the phase lag on the mismatch between the sols used. Accordingly, the top-most
 195 piece of the mole is at a depth of 5.07 ± 0.25 mm and the thermal diffusivity is $2.30 \pm$
 196 0.03×10^{-8} m² s⁻¹. Considering the radius of the mole of 13.5 mm and its inclination
 197 towards vertical of $30 \pm 0.2^\circ$, the center of the back-cap is at a depth of 11.8 ± 0.3 mm.
 198 The thermal skin depth is found to be 25 ± 0.4 mm and the wavelength 160 mm. The
 199 uncertainties of the measurements are detailed in the Supporting Information Text S2.

200 The data for the annual wave are significantly noisier than the diurnal wave record-
 201 ings, which should partly be a consequence of the weather on Mars. A total of 1.81 Mar-
 202 tian years (1231 sols) of surface temperatures are available but only 565 sols (0.85a) of
 203 buried mole data and only 459 sols (0.69a) after the Free Mole Test with the final ham-
 204 mering (compare Fig. 2). For the first year, surface temperatures were recorded over 24h
 205 at a coverage varying between 2 and 5700 recordings per sol. For the second year, data
 206 were regularly taken at 6:00 and 13:00 LTST to cover the daily minimum and maximum
 207 temperatures but only a few high time-resolution recordings could be afforded. There-
 208 fore, we use the 6:00 and 13:00 LTST recordings for the analysis (see Piqueux et al. (2021)
 209 for further advantages of using the RAD peak temperature values for thermophysical con-
 210 siderations). As a caveat we note that because of asymmetry in the daily surface tem-
 211 perature variation (compare Fig. S3 in the Supporting Information), the 24h temper-
 212 ature average and the average between the temperature extremes differed between 8 K
 213 during the cold season and 13 K during the warmest times. At mole depth, the temper-
 214 ature variation is significantly more symmetric and the difference between the 24h av-

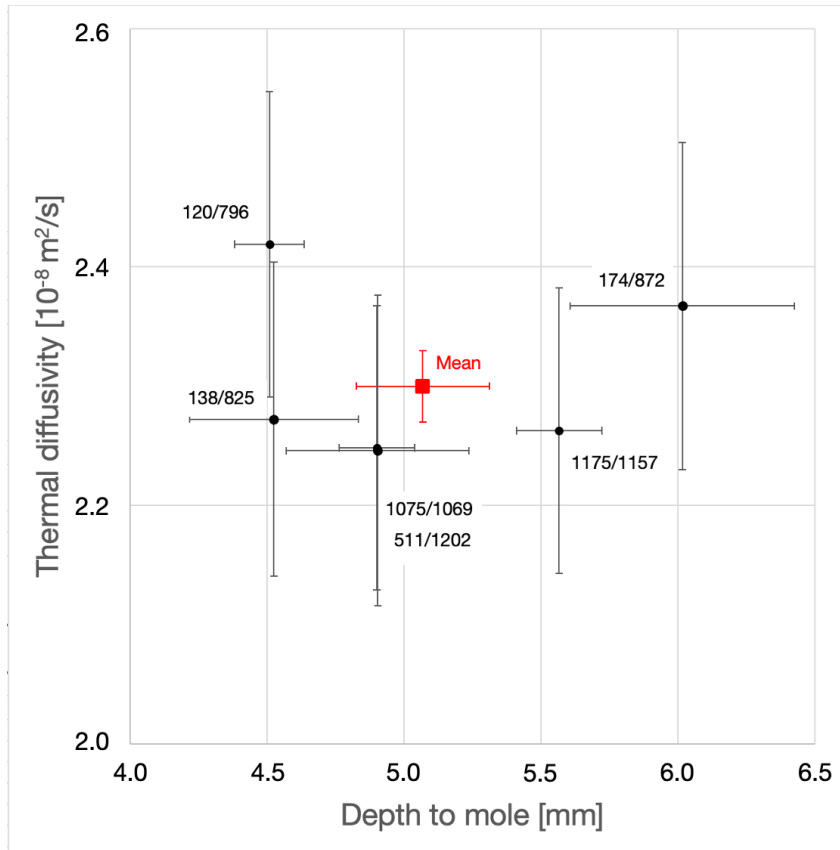


Figure 3. Thermal diffusivity versus depth to the back-end of the mole as calculated from the attenuation and the phase shift of the diurnal wave measured by the TEM-A sensor of the HP³ mole and the HP³ radiometer. The measurement uncertainties, the mean value and its standard error are indicated. The data points are marked by the combination of the sols used in the analysis.

215 erage and the average of the minimum and maximum temperatures is just a few tenth
 216 of a Kelvin.

217 The difference in temperature between the hottest day on the Martian surface and
 218 the coldest based on averaging the daily maximum and minimum temperatures was found
 219 to be 16.3K with an estimated uncertainty of 1K. At mole depth, 6 sols of high quality
 220 24h TEM-A data are available, complemented by re-calibrated housekeeping data of the
 221 mole motor temperature taken at 6:00 and 13:00 LTST. The annual temperature vari-
 222 ation at depth was found to be 13.2K, again with an estimated uncertainty of 1K. We
 223 estimate the phase shift between the surface and mole signal from a Fourier analysis of
 224 the signal. The analysis resulted in an estimate of the phase lag of 20.9 sols with an es-

225 timated uncertainty of ± 2 sols, an estimate somewhat more conservative than the dis-
 226 cretization uncertainty of ± 1.3 sols. This should accommodate for the contribution of
 227 the uncertainty in the amplitude to the uncertainty in the phase difference.

228 Attempts to use both the phase lag and the amplitude ratio to estimate κ and z_0
 229 as with the diurnal wave have proven to be impractical as the relative uncertainty for
 230 z_0 turned out to be several 100% in that case. Instead, we used the value of the depth
 231 to the mole determined from the diurnal wave and its uncertainty to estimate κ using
 232 the amplitude ratio and the phase lag separately. From the amplitude ratio we found
 233 κ to be $3.68 \pm 1.1 \times 10^{-8}$ W/m² and $3.80 \pm 0.51 \times 10^{-8}$ W/m² from the phase lag. Taking
 234 the average value of the two, we calculate a thermal skin depth of 84 ± 10 cm and a wave-
 235 length of 5.3 m.

236 3 Discussion and Conclusions

237 We have recorded the soil temperature measured by sensors on the HP³ mole as
 238 a function of time during 7 sols as well as during 4/5 of a Martian year. By comparing
 239 the mole temperature with the surface temperature we find a depth to the center of the
 240 mole back-end of 1.2 cm using the diurnal thermal wave. The thermal diffusivity was
 241 found to be $2.30 \pm 0.09 \times 10^{-8}$ m²/s². Using the annual wave data we find a thermal dif-
 242 fusivity of $3.74 \pm 0.61 \times 10^{-8}$ m²/s, suggesting that the thermal diffusivity increases with
 243 depth. Independent estimates of the thickness of the layer above the back-end of the mole
 244 from camera data taken during burial and tamping suggest a 1-2 cm (Spohn, Hudson,
 245 Marteau, et al., 2022) thick layer of sand/dust above the mole. The average thermal con-
 246 ductivity reported by Grott et al. (2021) is $k = 0.039 \pm 0.002$ W/m K and the density
 247 1211^{+149}_{-113} kg/m³. Assuming a heat capacity c as given by Morgan et al. (2018) of 630 J/kg K,
 248 a thermal diffusivity $\kappa = k/\rho c$ of $5.1 \pm 0.8 \times 10^{-8}$ m²/s (not counting the error in the heat
 249 capacity) is calculated. While the diurnal wave can be considered to sample the top few
 250 cm of the regolith where the thermal conductivity is likely to be smaller than in the layer
 251 below (Spohn, Hudson, Marteau, et al., 2022; Mueller et al., 2021; Piqueux et al., 2021),
 252 the annual wave and the TEM-A thermal conductivity measurement should cover a sim-
 253 ilar depth range, albeit with the annual wave penetrating several mole lengths deeper.
 254 While the thermal diffusivity values differ, it is fair to say that their 1- σ confidence ranges
 255 overlap. We further note that the present value is close to the pre-mission estimate by
 256 Morgan et al. (2018).

257 A representative average value of the temperature is 217.5 K with diurnal varia-
 258 tions of 5 to 7K and seasonal variations of 13K, respectively. The question arises for which
 259 depth or depth range the estimation should be considered representative, noting that tem-
 260 perature generally varies with depth in the Martian soil. The measurements of the TEM-
 261 A sensors give values averaged over at least the depth extent of the sensor foils, if not
 262 over the depth extent of the entire mole. The thermal conductivity of the mole is more
 263 than 10 times larger than that of the soil suggesting that the mole is close to isother-
 264 mal. Given that a TEM-A foil is 31.5cm long and that the tilt of the mole is 30°, their
 265 depth extent will be 27.3cm. With a depth to the back-end of the mole in its final con-
 266 figuration of 1.2cm and a mole length of 40 cm, the mole tip is at a depth of 36 cm. Since
 267 the H/K sensor is at 17.3cm distance from the back-end, it is at a depth of 16.2cm be-
 268 low the datum while the mid-point of the TEM-A foil is at 17.2cm depth. The center
 269 of the mole is at a depth of 19.2cm.

270 Another way to approach the problem is by considering the damping of the daily
 271 and annual thermal waves and finding the depth at which the recorded temperature and
 272 its diurnal and annual variation may be expected. By considering the exponential de-
 273 crease of the peak-to-peak temperature variation we find for an amplitude ratio of 0.06
 274 for the diurnal wave a representative depth of 7cm. For the annual wave with an am-
 275 plitude ratio of 0.81 a representative depth of 17 cm results. Assuming a Martian sur-
 276 face heat flow of 20 mW/m² (Plesa et al., 2018; Khan et al., 2021; Drilleau et al., 2022)
 277 and a thermal conductivity of 0.03-0.04 W/m K, consistent with the present value of κ
 278 and Grott et al. (2021), a thermal gradient of 0.5-0.7K/m results, suggesting a temper-
 279 ature difference between the two representative depths quoted above of less than 0.1K,
 280 smaller than the uncertainty range of even the high quality TEM-A data. We can use
 281 the gradient to estimate the temperature increase through the top 5m of the regolith to
 282 obtain 3K and a bottom temperature of 220.5K.

283 The average temperature value of 217.5K is 1 - 2K above the values given by Grott
 284 et al. (2007), lending support to the validity of this type of thermal models. These au-
 285 thors have assumed thermal diffusivity values between 1 and 2×10^{-8} m²/s and 2×10^{-8}
 286 m²/s and used the NASA/MSFC Mars GRAM model (Haberle et al., 1993) for the sur-
 287 face temperature. It is about 55 K below the melting temperature of pure ice I and 45 K
 288 below the triple point of the "average Mars salinity water" of Jones et al. (2011). It is
 289 about 20 K above the H₂O-Ca(ClO₄)₂ eutectic and above the sublimation temperature

290 of ice at Martian atmosphere pressure. This confirms the notion that the Martian soil
291 at Homestead Hollow should be desiccated as is to be expected for low latitude regions
292 on Mars (e.g., Clifford et al., 2010). In general, estimates of the depth to and the thick-
293 ness of the cryosphere may need revision though, given that our estimates of the ther-
294 mal diffusivity are about a factor of two lower than assumed for the near surface regolith
295 from previous studies (e.g., Clifford et al., 2010). Replacing their thermal conductivity
296 value of 0.06 W/m K with the one calculated here results in an estimated depth to the
297 bottom of the cryosphere smaller by 150m, or by 5%.

298 Jones et al. (2011) discuss a phase space for liquid water on Mars to evaluate the
299 astrobiological potential of the planet. As an upper estimate of the surface temperature
300 on Mars they use a value of 305K based on observations of the Opportunity rover at Merid-
301 iani Planum. We note that similar values of surface temperature have been observed by
302 HP³ RAD - for instance 295K on sol 1202 - but that night temperatures have then fallen
303 to values around 200K and that the temperature in the soil stayed well below the freez-
304 ing temperature of water even in the afternoon (compare Fig. 2).

305 Deliquescence of brines in thin films may be more realistic and has been suggested
306 for the Phoenix landing site (e.g., Chevrier et al., 2009; Rennó et al., 2009). For deliques-
307 cence to occur, the temperature must be above the eutectic of the brine and the humid-
308 ity above the deliquescence relative humidity (e.g., Nuding et al., 2014). Pál and Keresz-
309 turi (2020) have discussed the potential for deliquescence of three brines including cal-
310 cium perchlorate at Elysium Planitia, the wider region of the InSight landing site. They
311 find about 2h long intervals of favourable conditions for the formation of calcium per-
312 chlorate brines in the evening between 21:00 and 23:00 LTST in early spring. We note
313 that the conditions in the soil at a depth of about 10cm (and beyond) would be driven
314 by the humidity as the temperature should be continuously above the eutectic of the cal-
315 cium perchlorate brine of around 200K (Nuding et al., 2014). Judging from the model
316 of Pál and Kereszturi (2020), the brine could exist for about 10h, a conclusion similar
317 to the finding of Nuding et al. (2014) for the Phoenix landing site albeit for a depth of
318 3cm, there. At 3cm depth, the time window for deliquescence at Homestead Hollow should
319 be shorter as the temperature should fall below the eutectic at around 6:00 LTST.

320 Efflorescence of salt from the supersolidus brine may well have caused the forma-
321 tion of the about 20cm thick duricrust that hampered the mole progress as reported in

322 Spohn, Hudson, Witte, et al. (2022) and Spohn, Hudson, Marteau, et al. (2022). Chem-
323 ical measurements of soils and alteration rinds of rocks argue for low water/rock ratio
324 alteration due to acidic weathering via interactions of atmospheric water vapor and soils
325 to produce chlorine and sulfur rich salts that cement near surface soils and duricrusts
326 on Mars (Banin et al., 1992; Haskin et al., 2005; Hurowitz et al., 2006, 2007).

327 **4 Open Research**

328 Calibrated HP³ radiometer and TEM-A data are archived in NASA’s Planetary
329 Data System (InSight HP³ Science Team, 2021). The specifically selected data, the house-
330 keeping sensor data and the Excel workbooks used to evaluate the data have been made
331 publicly available at Spohn (2024).

332 **Acknowledgments**

333 The design, building of and research into the HP³ has been supported by the German
334 Aerospace Center DLR, by NASA, the ÖAW, and the Polish Academy of Science. A por-
335 tion of the work was supported by the InSight Project at the Jet Propulsion Laboratory,
336 California Institute of Technology, under a contract with the National Aeronautics and
337 Space Administration (80NM0018D0004).

338 This is InSight contribution number 337.

339 **References**

- 340 Banerdt, W. B., Smrekar, S. E., Banfield, D., Giardini, D., Golombek, M., John-
341 son, C. L., ... Wieczorek, M. (2020). Initial results from the InSight mission
342 on Mars. *Nature Geoscience*. Retrieved from [https://doi.org/10.1038/
343 s41561-020-0544-y](https://doi.org/10.1038/s41561-020-0544-y) doi: 10.1038/s41561-020-0544-y
- 344 Banin, A., Clark, B. C., & Waenke, H. (1992). Surface Chemistry and Mineralogy.
345 In H. Kieffer, B. Jakosky, C. Snyder, & M. Matthews (Eds.), *Mars* (p. 594-
346 625.). Tucson: Univ. Arizona Press.
- 347 Boston, P., Todd, P., Camp, J., Northup, D., & Spilde, M. (2009, September). Mars
348 simulation challenge experiments: Microorganisms from natural rock and cave
349 communities. In *Gravitational and space biology* (Vol. 22(2), p. 39-44).
- 350 Carslaw, H. S., & Jaeger, J. (1959). *Conduction of heat in solids, 2nd ed.* Oxford:
351 Oxford University Press.

- 352 Chevrier, V. F., Hanley, J., & Altheide, T. S. (2009). Stability of perchlorate hy-
 353 drates and their liquid solutions at the Phoenix landing site, Mars. *Geophysical*
 354 *Research Letters*, *36*(10).
- 355 Clifford, S. M., Lasue, J., Heggy, E., Boisson, J., McGovern, P., & Max, M. D.
 356 (2010). Depth of the martian cryosphere: Revised estimates and implica-
 357 tions for the existence and detection of subpermafrost groundwater. *Jour-*
 358 *nal of Geophysical Research: Planets*, *115*(E7). Retrieved from [https://](https://agupubs.onlinelibrary.wiley.com/doi/abs/10.1029/2009JE003462)
 359 agupubs.onlinelibrary.wiley.com/doi/abs/10.1029/2009JE003462 doi:
 360 <https://doi.org/10.1029/2009JE003462>
- 361 Cockell, C. S. (2014). 11. the subsurface habitability of terrestrial rocky planets:
 362 Mars. In J. Kallmeyer & D. Wagner (Eds.), *Microbial life of the deep biosphere*
 363 (pp. 225–260). Berlin, Boston: De Gruyter. doi: doi:10.1515/9783110300130
 364 .225
- 365 Drilleau, M., Samuel, H., Garcia, R. F., Rivoldini, A., Perrin, C., Michaut, C., ...
 366 Banerdt, W. B. (2022). Marsquake locations and 1-D seismic models for
 367 Mars from InSight data. *Journal of Geophysical Research: Planets*, *127*(9),
 368 e2021JE007067. doi: <https://doi.org/10.1029/2021JE007067>
- 369 Golombek, M., Warner, N. H., Grant, J. A., Hauber, E., Ansan, V., Weitz, C. M.,
 370 ... Banerdt, W. B. (2020). Geology of the InSight landing site on Mars.
 371 *Nature Communications*, *11*, 1014. doi: 10.1038/s41467-020-14679-1
- 372 Grott, M., Helbert, J., & Nadalini, R. (2007). Thermal structure of Martian soil and
 373 the measurability of the planetary heat flow. *Journal of Geophysical Research*
 374 (*Planets*), *112*(E9), E09004. doi: 10.1029/2007JE002905
- 375 Grott, M., Piqueux, S., Spohn, T., Knollenberg, J., Krause, C., Marteau, E., ...
 376 Banerdt, W. B. (2023). Seasonal variations of soil thermal conductivity at
 377 the InSight landing site. *Geophysical Research Letters*, *50*(7), e2023GL102975.
 378 Retrieved from [https://agupubs.onlinelibrary.wiley.com/doi/abs/](https://agupubs.onlinelibrary.wiley.com/doi/abs/10.1029/2023GL102975)
 379 [10.1029/2023GL102975](https://doi.org/10.1029/2023GL102975) doi: <https://doi.org/10.1029/2023GL102975>
- 380 Grott, M., Spohn, T., Knollenberg, J., Krause, C., Hudson, T. L., Piqueux, S., ...
 381 Banerdt, W. B. (2021, July). Thermal conductivity of the Martian soil at
 382 the InSight landing site from HP³ active heating experiments. *Journal of*
 383 *Geophysical Research (Planets)*, *126*(7), e06861. doi: 10.1029/2021JE006861
- 384 Grott, M., Spohn, T., Knollenberg, J., Krause, C., Scharringhausen, M., Wipper-

- 385 mann, T., ... Banerdt, W. B. (2019). Calibration of the Heat Flow and
 386 Physical Properties Package (HP³) for the InSight Mars Mission. *Earth and*
 387 *Space Science*, 6(12), 2556-2574. doi: 10.1029/2019EA000670
- 388 Haberle, R. M., Pollack, J. B., Barnes, J. R., Zurek, R. W., Leovy, C. B., Mur-
 389 phy, J. R., ... Schaeffer, J. (1993, February). Mars atmospheric dynamics
 390 as simulated by the NASA Ames General Circulation Model. 1. The zonal-
 391 mean circulation. *Journal of Geophysical Research*, 98(E2), 3093-3123. doi:
 392 10.1029/92JE02946
- 393 Haskin, L., Wang, A., Bradley, L., & et al. (2005). Water alteration of rocks and
 394 soils on Mars at the Spirit rover site in Gusev crater. *Nature*. doi: 10.1038/
 395 nature03640
- 396 Hillel, D. (2001). Soil Physics. In R. A. Meyers (Ed.), *Encyclopedia of physical sci-*
 397 *ence and technology 3rd ed, earth sciences* (p. 77 - 97). Cambridge: Academic
 398 Press.
- 399 Hurowitz, S., McLennan, S., Tosca, N., & et al. (2006). In situ and experimental ev-
 400 idence for acidic weathering of rocks and soils on Mars. *J. Geophys. Res.*. doi:
 401 10.1029/2005JE002515
- 402 Hurowitz, S., McLennan, S., Tosca, N., & et al. (2007). A 3.5 Ga record of water-
 403 limited, acidic weathering conditions on Mars. *EPSL*, 260, 432-443. doi: 10
 404 .1016/j.epsl.2007.05.043.10.1029/2005JE002515
- 405 InSight HP³ Science Team. (2021). *Mars InSight Lander HP³ Data Archive*
 406 *[Dataset]*. NASA Planetary Data System. doi: 10.17189/1517573
- 407 Jones, E., Lineweaver, C., & Clarke, J. (2011, 12). An extensive phase space for the
 408 potential Martian biosphere. *Astrobiology*, 11, 1017-33. doi: 10.1089/ast.2011
 409 .0660
- 410 Khan, A., Ceylan, S., van Driel, M., Giardini, D., Lognonné, P., Samuel, H.,
 411 ... Banerdt, W. B. (2021). Upper mantle structure of Mars from
 412 InSight seismic data. *Science*, 373(6553), 434-438. Retrieved from
 413 <https://www.science.org/doi/abs/10.1126/science.abf2966> doi:
 414 10.1126/science.abf2966
- 415 Lemmon, M. T., Wolff, M. J., Bell, J. F., Smith, M. D., Cantor, B. A., & Smith,
 416 P. H. (2015). Dust aerosol, clouds, and the atmospheric optical depth record
 417 over 5 Mars years of the Mars Exploration Rover mission. *Icarus*, 251, 96-111.

- 418 doi: <https://doi.org/10.1016/j.icarus.2014.03.029>
- 419 Morgan, P., Grott, M., Knapmeyer-Endrun, B., Golombek, M., Delage, P.,
420 Lognonné, P., . . . Kedar, S. (2018). A pre-landing assessment of regolith
421 properties at the InSight landing site. *Space Science Reviews*, 214(6), 104. doi:
422 10.1007/s11214-018-0537-y
- 423 Mueller, N. T., Knollenberg, J., Grott, M., Kopp, E., Walter, I., Krause, C., . . . Sm-
424 rekar, S. (2020). Calibration of the HP³ Radiometer on InSight. *Earth and*
425 *Space Science*, 7(5), e01086. doi: 10.1029/2020EA001086
- 426 Mueller, N. T., Piqueux, S., Lemmon, M., Maki, J., Lorenz, R., Grott, M., . . .
427 Banerdt, W. (2021). Near surface properties derived from Phobos transits
428 with HP³ RAD on InSight, Mars. *Geophysical Research Letters*, 48. doi:
429 <https://doi.org/10.1029/2021GL093542>
- 430 Nuding, D., Rivera-Valentin, E., Davis, R., Gough, R., Chevrier, V., & Tolbert, M.
431 (2014). Deliquescence and efflorescence of calcium perchlorate: An investi-
432 gation of stable aqueous solutions relevant to Mars. *Icarus*, 243, 420-428.
433 Retrieved from [https://www.sciencedirect.com/science/article/pii/](https://www.sciencedirect.com/science/article/pii/S0019103514004527)
434 [S0019103514004527](https://www.sciencedirect.com/science/article/pii/S0019103514004527) doi: <https://doi.org/10.1016/j.icarus.2014.08.036>
- 435 Piqueux, S., Mueller, N., Grott, M., Siegler, M., Millour, E., Forget, F., . . . Banerdt,
436 W. (2021). Soil thermophysical properties near the InSight Lander derived
437 from 50 sols of radiometer measurements. *Journal of Geophysical Research*
438 *(Planets)*, 126. doi: <https://doi.org/10.1029/2021JE006859>
- 439 Plesa, A.-C., Padovan, S., Tosi, N., Breuer, D., Grott, M., Wieczorek, M. A., . . .
440 Banerdt, W. B. (2018). The thermal state and interior structure of Mars.
441 *Geophysical Research Letters*, 45(22), 12,198-12,209. Retrieved from [https://](https://agupubs.onlinelibrary.wiley.com/doi/abs/10.1029/2018GL080728)
442 agupubs.onlinelibrary.wiley.com/doi/abs/10.1029/2018GL080728 doi:
443 10.1029/2018GL080728
- 444 Pál, B., & Kereszturi, A. (2020). Annual and daily ideal periods for deliquescence
445 at the landing site of InSight based on GCM model calculations. *Icarus*, 340,
446 113639. Retrieved from [https://www.sciencedirect.com/science/article/](https://www.sciencedirect.com/science/article/pii/S0019103519304956)
447 [pii/S0019103519304956](https://www.sciencedirect.com/science/article/pii/S0019103519304956) doi: <https://doi.org/10.1016/j.icarus.2020.113639>
- 448 Rapp, D. (2023). *Human missions to mars* (3rd ed.). Heidelberg, Germany, New
449 York, USA: Springer.
- 450 Rennó, N. O., Bos, B. J., Catling, D., Clark, B. C., Drube, L., Fisher, D., . . . others

- 451 (2009). Possible physical and thermodynamical evidence for liquid water at the
452 Phoenix landing site. *Journal of Geophysical Research: Planets*, 114(E1).
- 453 Spohn, T. (2024). *Mars Soil Temperature and Thermal Diffusivity from InSight HP³*
454 *Data Workbook [Dataset, Software]*. FigShare.Collection. doi: 10.6084/m9
455 .figshare.25099754
- 456 Spohn, T., Grott, M., Smrekar, S. E., Knollenberg, J., Hudson, T. L., Krause, C.,
457 ... Banerdt, W. B. (2018, Aug 02). The Heat Flow and Physical Proper-
458 ties Package (HP³) for the InSight mission. *Space Science Reviews*, 214(5),
459 96. Retrieved from <https://doi.org/10.1007/s11214-018-0531-4> doi:
460 10.1007/s11214-018-0531-4
- 461 Spohn, T., Hudson, T. L., Marteau, E., Golombek, M., Grott, M., Wippermann, T.,
462 ... Banerdt, W. B. (2022). The InSight HP³ penetrator (Mole) on Mars: Soil
463 properties derived from the penetration attempts and related activities. *Space*
464 *Science Reviews*, 218. doi: <https://doi.org/10.1007/s11214-022-00941-z>
- 465 Spohn, T., Hudson, T. L., Witte, L., Wippermann, T., Wisniewski, L., Kedziora, B.,
466 ... Grygorczuk, J. (2022). The InSight-HP³ Mole on Mars: Lessons learned
467 from attempts to penetrate to depth in the Martian soil. *Advances in Space*
468 *Research*, 69, 3140-3163. doi: <https://doi.org/10.1016/j.asr.2022.02.009>
- 469 Trebi-Ollennu, A., Kim, W., Ali, K., Khan, O., Sorice, C., Bailey, P., ... Lin, J.
470 (2018). InSight Mars lander Robotics Instrument Deployment system. *Space*
471 *Sci Rev*, 214(93). doi: doi.org/10.1007/s11214-018-0520-7
- 472 Zent, A. P., Hecht, M. H., Cobos, D. R., Wood, S. E., Hudson, T. L., Milkovich,
473 S. M., ... Mellon, M. T. (2010). Initial results from the thermal and electrical
474 conductivity probe (TECP) on Phoenix. *Journal of Geophysical Research:*
475 *Planets*, 115(E3). doi: <https://doi.org/10.1029/2009JE003420>